Bedrock displacements in Greenland manifest ice mass variations, climate cycles and climate change

Michael Bevis[a,1], John Wahr[b], Shfaqat A. Khan[c], Finn Bo Madsen[c], Abel Brown[a], Michael Willis[d], Eric Kendrick[a], Per Knudsen[c], Jason E. Box[e], Tonie van Dam[f], Dana J. Caccamise II[a], Bjorn Johns[g], Thomas Nylen[g], Robin Abbott[h], Seth White[g], Jeremy Miner[g], Rene Forsberg[c], Hao Zhou[a], Jian Wang[a], Terry Wilson[a], David Bromwich[e], and Olivier Francis[f]

[a]School of Earth Sciences, Ohio State University, Columbus, OH 43210; [b]Department of Physics, University of Colorado, Boulder, CO 80309; [c]DTU Space, National Space Institute, Lyngby, Denmark; [d]Department of Earth and Atmospheric Sciences, Cornell University, Ithaca, NY 14853; [e]Department of Geography, Ohio State University, Columbus, OH 43210; [f]Faculté de Sciences, University of Luxembourg, Luxembourg; [g]UNAVCO Inc., Boulder, CO 80301; and [h]Polar Field Services, Boulder, CO 80127

Edited by David T. Sandwell, Scripps Institution of Oceanography, La Jolla, CA, and approved June 11, 2012 (received for review March 19, 2012)

The Greenland GPS Network (GNET) uses the Global Positioning System (GPS) to measure the displacement of bedrock exposed near the margins of the Greenland ice sheet. The entire network is uplifting in response to past and present-day changes in ice mass. Crustal displacement is largely accounted for by an annual oscillation superimposed on a sustained trend. The oscillation is driven by earth's elastic response to seasonal variations in ice mass and air mass (i.e., atmospheric pressure). Observed vertical velocities are higher and often much higher than predicted rates of postglacial rebound (PGR), implying that uplift is usually dominated by the solid earth's instantaneous elastic response to contemporary losses in ice mass rather than PGR. Superimposed on longer-term trends, an anomalous 'pulse' of uplift accumulated at many GNET stations during an approximate six-month period in 2010. This anomalous uplift is spatially correlated with the 2010 melting day anomaly.

climate change | climate cycles | elasticity | crustal motion geodesy

The Greenland GPS Network (GNET) (Figs. 1–3) was constructed during the 2007, 2008, and 2009 field seasons in order to develop a new means to measure the impact of climate cycles and climate change on ice mass balance in the world's second largest ice sheet. The primary objective of GNET is to "weigh" the Greenland ice sheet by measuring the earth's instantaneous elastic response to contemporary changes in ice mass (1), much as a traditional bathroom scale measures body mass by gauging the degree to which it can compress a spring. A secondary goal of GNET is to assess the rate of postglacial rebound (PGR)—i.e., the delayed viscoelastic response to past changes in ice mass—and so contribute to an improved "PGR correction" (2, 3) for Gravity Recovery and Climate Experiment (GRACE) (4) and its follow-on missions. A key challenge for GNET is distinguishing between the steady (i.e., constant velocity) component of elastic rebound and PGR. However, this potential ambiguity does *not* apply to non-steady elastic displacements driven by climate cycles (especially the annual cycle) or by accelerations in ice mass trends. PGR proceeds at effectively constant rates at annual and decadal timescales. Abrupt changes, oscillations, or sustained accelerations in bedrock uplift are unambiguous indicators of abrupt, oscillatory, or accelerating changes in the loads imposed upon the surface of the solid earth.

Before GNET was established, crustal displacement time series were available only at a handful of Global Positioning System (GPS) stations in Greenland (Fig. 4), and these were so far apart that it was impossible to infer the spatial variability of uplift in any detail. Now that GNET has been constructed, there are more than 50 GPS stations surrounding the Greenland ice sheet. All of these new stations have their antennas firmly attached to bedrock, and thus faithfully record crustal motion. We have analyzed these measurements (*SI Appendix*, section 1) and now present our first geodetic analysis of crustal displacement across GNET. To a first approximation, the vertical displacement histories at GNET stations established during or after the summer of 2007 are well explained by a constant velocity model. The same is true of most but not all of the older GPS stations (Fig. 4). The average rates of bedrock uplift observed by GNET up until epoch 2011.25 (Figs. 1–3) exceed and often greatly exceed the rates predicted by leading PGR models (5–9) (*SI Appendix*, section 2). For example, the median difference (across GNET) between observed vertical velocities and the PGR rates predicted by the model ICE5G VM2 (6) is +8.2 mm/yr. The maximum difference (GPS—predicted PGR) is >31 mm/yr. Observed coastline-perpendicular gradients in uplift rate also greatly exceed those predicted by all leading PGR models. This implies that elastic rebound at least matches and usually dominates PGR over most of coastal Greenland.

This conclusion is supported by the fact that the most rapidly uplifting stations are located in northwest and southeast Greenland, where GRACE has recorded the greatest loss of ice mass since GNET began (10, 11). Some care must be taken in interpreting our vertical velocity field (Figs. 1–3) because local uplift rates within Greenland are not always steady, so a GPS station's average velocity may vary according to the time span of observation (Fig. 4*B*), which can change in space from one station to the next (*SI Appendix*, Table S1). Previous studies (10–12) have demonstrated that the three longest-lived GPS stations in Greenland (KELY, KULU, and THU1/2/3) have all recorded large changes in uplift rate during their lifetimes. (Note that stations THU2 and THU3 actually refer to the same GPS antenna. We process both data sets but normally present the results from the THU2 receiver since it has the longer time series). The accelerations observed at THU2 and KULU since 2002 are broadly consistent with the space–time changes in ice mass inferred from GRACE (10, 11). Since these accelerations are clearly resolved only over time periods of approximately three years or more, similar patterns of acceleration would be hard to detect using GNET stations with observational timespans of less than three years. However, the 2010 melting day anomaly (13), which was particularly intense in southern Greenland, has provided us with a new opportunity to demonstrate the utility of GNET as a regional ice mass sensing system. A melting day anomaly is defined as the number of extra days of melting that occur in a given year,

Author contributions: M.B., F.B.M., P.K., T.v., D.J.C., and T.W. designed research; M.B., S.A.K., F.B.M., A.B., M.W., E.K., D.J.C., B.J., T.N., R.A., S.W., J.M., R.F., H.Z., J. Wang, and O.F. performed research; J.E.B. and D.B. contributed new analytic tools; M.B., J. Wahr, A.B., and E.K. analyzed data; and M.B., J. Wahr, and S.A.K. wrote the paper;.

The authors declare no conflict of interest.

This article is a PNAS Direct Submission.

Freely available online through the PNAS open access option.

[1]To whom correspondence may be addressed. Email: mbevis@osu.edu or mbevis@gmail.com.

This article contains supporting information online at www.pnas.org/lookup/suppl/doi:10.1073/pnas.1204664109/-/DCSupplemental.

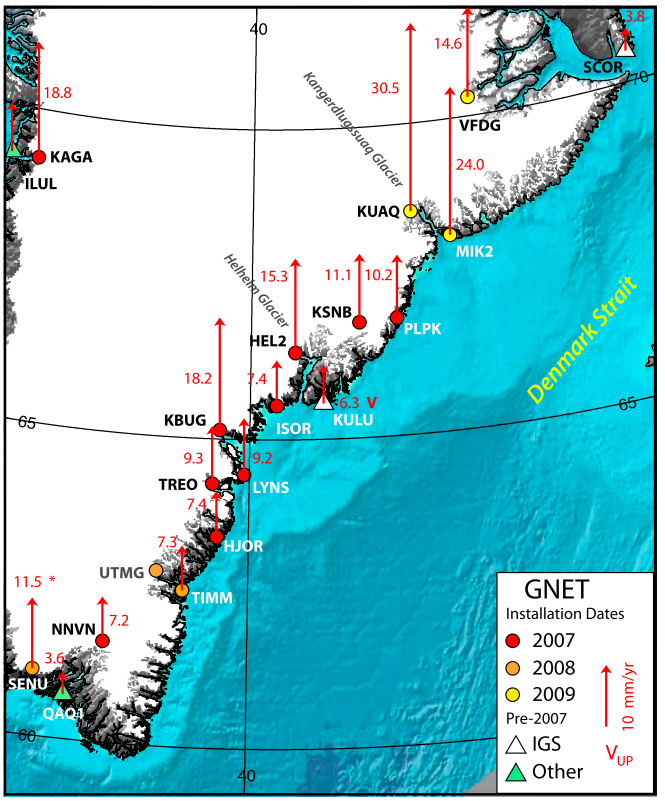

Fig. 1. Observed vertical velocities (in mm/yr) of the GNET stations in southeast Greenland. These velocities, their uncertainties (<1 mm/yr), and the observational time spans are listed in *SI Appendix*, Table S1. When a station's velocity estimate is known to have been very strongly affected by the 2010 ice loss anomaly (as at station SENU), the velocity label is marked *. However, there is no way to know the extent to which the 2010 anomaly has affected the GNET stations established in 2009. Some of the longer-lived GPS stations such as KULU have recorded major changes in uplift rate throughout their lifetimes, in which case their average vertical velocity since the beginning of year 2000 is given, and this velocity is marked with a V to indicate multiyear variability. Note that station symbols encode their installation dates. The highest uplift rates observed so far anywhere in Greenland are those at stations MIK2 and KUAQ; however, it seems likely that these rates were perturbed upwards by the 2010 melting anomaly, and do not represent the average uplift rates over the several years prior to 2010.

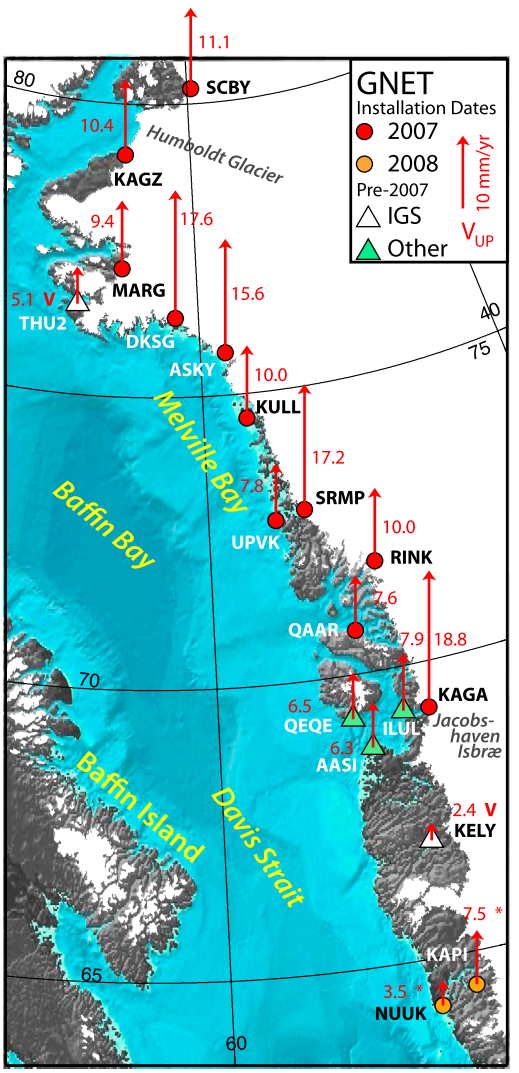

Fig. 2. Observed vertical velocities in west and northwest Greenland. Symbols and related information are explained in the caption to Fig. 1. Note that, in a given section of the coastal region, station velocity tends to increase as distance to the ice margin decreases. One sigma standard errors are nearly always <1 mm/yr (*SI Appendix*, Table S1).

relative to a long-term average number of days per year that melting occurs in that location (13). The record-breaking summer of 2010 was unusually long as well as unusually hot, and it produced one of the largest melting day anomalies ever observed in Greenland. We shall show that GNET recorded this event and confirms that an unusually large loss of ice mass occurred in Greenland during the extended melting season of 2010.

Analysis

Crustal Motion Analysis. The phenomenology of crustal motion in Greenland is surprisingly rich. We model the upwards component of displacement (U) at each GPS station as a combination of a secular trend and an annual oscillation (Fig. 4*A*). The trend is modeled as a polynomial function of time and the oscillation is approximated using a four-term Fourier series (FS) composed of annual and semiannual harmonics (*SI Appendix*, section 1). We defer discussion of cycles to a later section of this paper, and focus for now on the trends. We are required to invoke quadratic and cubic trends at THU2 and KULU, respectively, in order to obtain a reasonable fit to their time series, whereas the other stations in Fig. 4*A* are well modeled using a linear (constant velocity) trend, at least up to approximately 2010.4. [Though when older (pre-2000) data from KELY are included, it is necessary to use a quadratic model to retain a good fit (12), even if we exclude measurements made after 2010.4.] After approximately 2010.4, the vertical time series systematically deviate from their trajectory models at every long-lived station except THU2 in Thule, northwest Greenland (Fig. 4*A*).

This anomalous "pulse" of uplift underlines the need to interpret the average vertical velocities recorded by GNET stations with some care. If we were to estimate uplift rates at any GPS station in Fig. 4*A* except THU2 using only the observations obtained in 2009 and 2010, we would obtain far higher velocities than if we used all available data, as seen in Fig. 4*B*. For $t < 2010.4$, the vertical displacement history, U(t), at every GNET station established in 2007 or thereafter can be well modeled using a linear or constant-velocity trend. But after the onset of the anomalous 2010 melting season, it soon becomes necessary to model U(t) at many of these GNET stations using a higher-order polynomial trend, or to regard U(t) as being composed of a linear trend plus an anomalous pulse of uplift that accumulated in an approximate six-month period in 2010. Since the 2010 melting anomaly is probably a discrete event, rather than the onset of a new long-term trend, we take the second approach here.

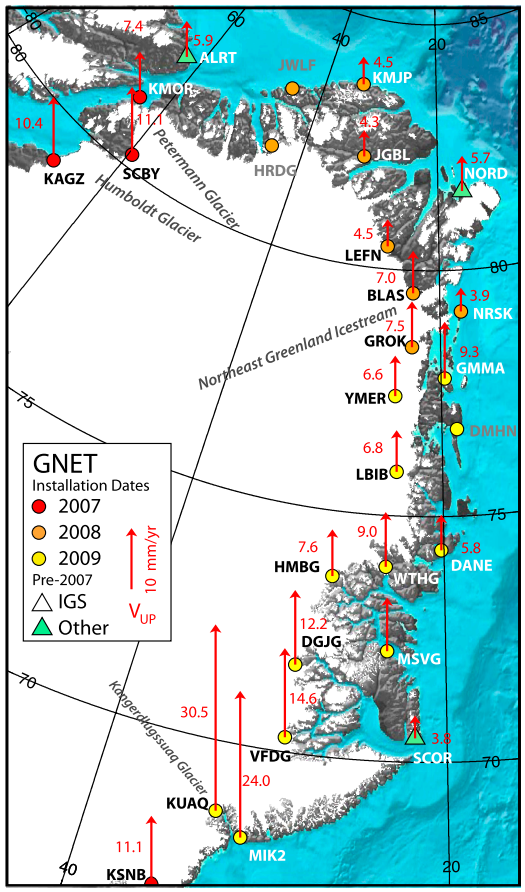

Fig. 3. Observed vertical velocities in north and northeast Greenland. Symbols and related information are explained in the caption to Fig. 1. Here, as in Figs. 1 and 2, if the four-letter station code appears in grey it means that a velocity solution is not yet available because technical problems led to a total observational timespan of less than one year. The standard error estimates for velocity vary with the timespan of observation (*SI Appendix*, Table S1) but are nearly always <1 mm/yr.

The 2010 Uplift Anomaly. We can estimate the 2010 uplift anomaly at many of the GNET stations established before 2009 by fitting a trend-plus-oscillation model to the time series prior to 2010.4, extrapolating this model to the end of our time series (2011.25), and averaging the difference between the observed and predicted U coordinate in the interval 2010.8–2011.25 (Fig. 4*B*). Unfortunately, we cannot estimate the uplift anomaly that occurred at the GNET stations established in 2009 because the time series available prior to the onset of anomalous uplift is too short to establish a model for the normal pattern of displacement prior to approximately 2010.4. Data gaps prevented us from estimating the uplift anomaly at several additional stations. We were able to gauge the 2010 uplift anomaly at 32 GNET stations, and these estimates are depicted in Fig. 5, along with a representation of the spatial development of the 2010 melting day anomaly (13). The spatial correlation between these anomalies is obvious once we take into account the tendency for earth's elastic response to ice loss to decrease with increasing distance from the loss center (i.e., the ice margin). Note that the two stations with the most negative uplift anomalies (THU2 and DKSG) are located in areas with negative melting day anomalies that are not offset by nearby zones with strongly positive melting day anomalies (Fig. 5). We concede that our estimate of the 2010 uplift anomaly is imperfect in that we did not use the same baseline period at every station in order to define "normal" (and thus "anomalous") displacements. This problem—derived from inhomogeneity of temporal coverage—will recede as GNET ages.

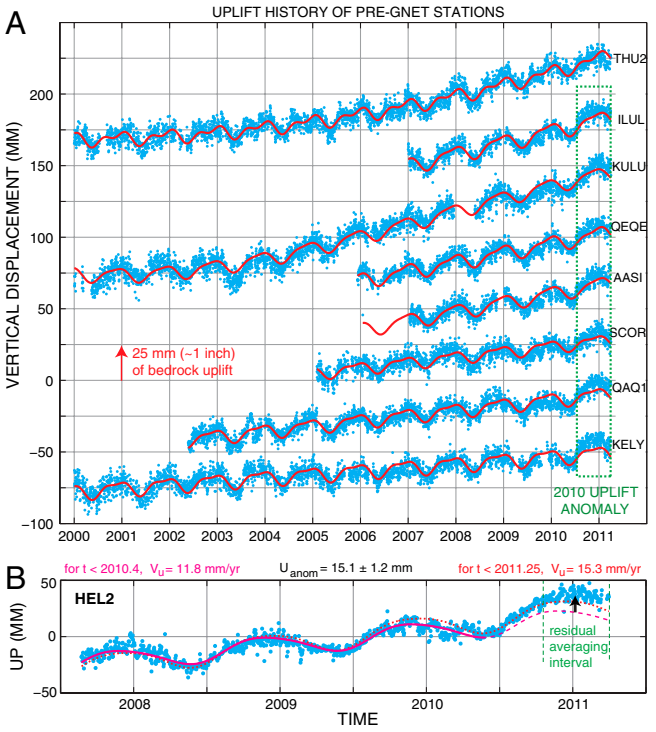

Fig. 4. (*A*) Vertical displacement time series at selected older GPS stations (blue dots) and model trajectory (red) curves composed of an annual oscillation plus a multiyear trend. The trend model is linear in time except at stations THU2 and KULU, where it is a second- and third-order polynomial, respectively. Note that for every station shown except THU2, the model curve systematically underestimates the observations obtained after approximately 2010.4. (*B*) The vertical displacement times series U(t) (blue dots) at HEL2. A trajectory model fit to U(t) for $t < 2010.40$ (solid magenta line) is projected to the end of the time series at 2011.25 (dashed magenta line). The 2010 uplift anomaly is defined as the mean difference between the U(t) and this projected curve during the time interval 2010.8–2011.25. This anomaly (15.2 ± 12 mm) is indicated by the black arrow. The velocity of the trend established prior to 2010.4 is 11.8 mm/yr. But if a trajectory model is fit to all U(t)—i.e., for $t < 2011.25$ (red dotted curve)—then the velocity changes to 15.3 mm/yr.

The summer of 2010 was the hottest and longest on record over most of southern Greenland. In many areas there was also lower than normal snowfall in 2010, which locally added to a negative surface mass balance (SMB) anomaly (13). No major increases in discharge rate were observed at the three largest glaciers during 2010 (14). Despite the limitations of our estimation technique, there can be very little doubt that GNET sensed an anomalous pulse of ice loss during the extended melting season of 2010 (Fig. 5).

The 2010 Mass Anomaly. We can use GRACE to estimate a 2010 mass anomaly in much the same way that we estimated the uplift anomaly using GNET time series. Monthly average GRACE measurements tend to scatter around a best-fit multiyear trend plus oscillation model with higher scatter levels than are associated with monthly average uplift measurements. Therefore, to improve the stability of the mass anomaly estimates (for the 2010 melting season), we divide Greenland into just two zones (north and south of 72.2 °N) and make no attempt to resolve the spatial structure of the mass anomaly in more detail. We estimate the mass anomalies accumulated between 2010.4 and 2010.79 to be -113 ± 28 GT (1 GT = 10^{12} kg) in southern Greenland and $+32 \pm 28$ GT in northern Greenland (*SI Appendix*, section 3). While the anomalous mass gain in northern Greenland is barely significant at the 2-sigma level, the anomalous mass loss in southern Greenland is highly significant. While both GRACE

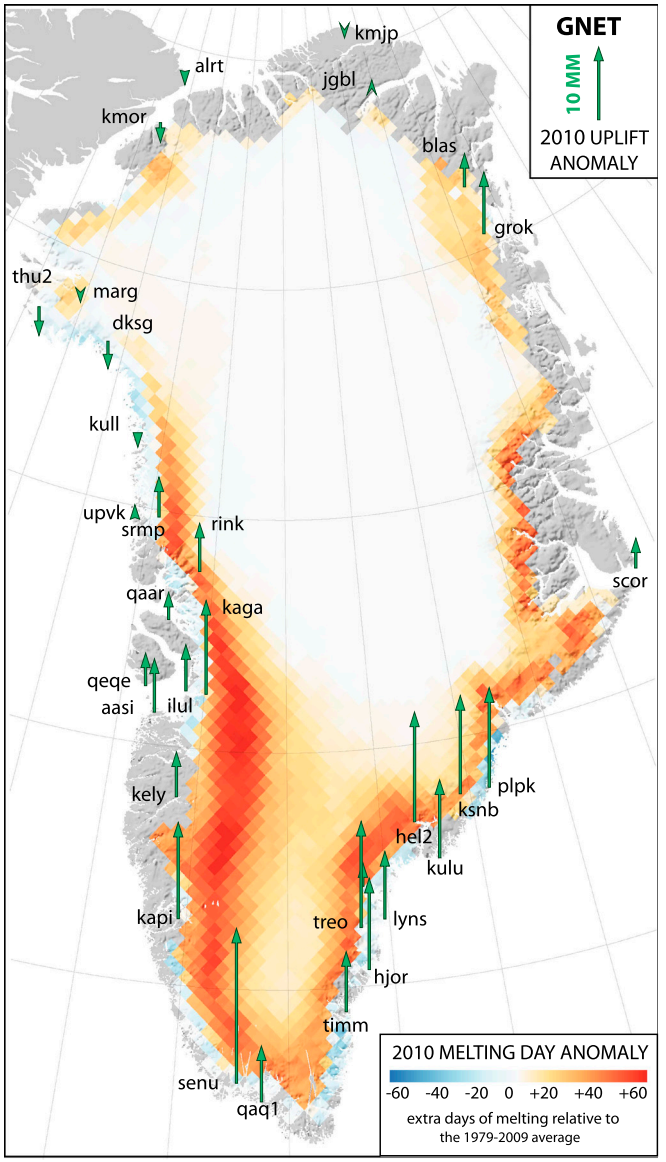

Fig. 5. The 2010 uplift anomaly (green arrows) for all GPS stations in Greenland where it could be reliably computed, superimposed on a map showing the 2010 melting day anomaly that was produced by R. Simmon at the NASA Earth Observatory using data provided by M. Tedesco (13). When we take into account the tendency for the earth's elastic response to ice loss to decrease with distance from the unloading area (i.e., the ice margin), then the spatial correlation between the uplift anomaly and the melting day anomaly is apparent. The standard errors associated with the 2010 uplift anomaly estimates are listed in *SI Appendix*, Table S2. They are typically close to approximately 1.75 mm.

and GNET agree that anomalous mass loss in mid and late 2010 was concentrated in the south of Greenland, the average displacement anomaly sensed by GNET in northern Greenland was close to zero, whereas GRACE suggests a modest mass gain in this zone. This discrepancy could be explained if most of the mass gain occurred in the interior of northern Greenland, since GRACE is more sensitive to mass change in the interior than near the margins (*SI Appendix*, section 3), whereas the reverse is true of the GPS stations, and to an even greater degree (11).

Seasonal Cycles. GPS displacement time series exhibit annual oscillations all over the world (15), especially in the vertical component. These displacement cycles are very evident in Greenland (Fig. 4), but at first glance they seem enigmatic because the bedrock uplift cycle always peaks at least several months after the ice mass cycle reaches its minimum in late summer. We now demonstrate that this is because the displacement cycle is responding to seasonal changes in air mass as well as ice mass. In Fig. 6 we show the average GNET displacement cycle and compare it to seasonal cycles in ice mass and air mass overlying Greenland as a whole. The ice mass cycle was estimated from GRACE: we fitted the all-Greenland mass change time series (early 2002–early 2011) with a quadratic trend and a 4-term FS, and then isolated the oscillatory component. We note that this estimate for the ice mass cycle is in good accord with that determined from SMB-Discharge studies (16). We estimated the annual cycle in air mass using an 8-year time series of surface pressure fields produced by the mesoscale numerical weather model Polar MM5 (17). The seasonal variation of the air mass overlying Greenland was characterized using a 4-term FS, just as we handled the ice mass and displacement cycles. Note that the air mass cycle and the ice mass cycle have similar amplitudes but very different phase structure (Fig. 6). The sum of these two mass cycles constitutes the total annual loading cycle, and its shape far more closely corresponds to that of the crustal displacement cycle than do either of the individual mass cycles (Fig. 6). We do not expect a perfect agreement at this stage of our investigation, because there are still some uncertainties associated with our estimates for the ice mass and air mass cycles, and because the mean displacement cycle is based on an irregular sampling of Greenland while the mass cycle estimates are not. Our finding is something of a complication for GNET since it implies that we must routinely use pressure fields from numerical weather models to isolate the solid earth's response to seasonal ice mass variations. But this complication is also a blessing in that GPS position determinations are made daily, and we should be able to use the correlation between daily displacements and daily average surface pressure fields to calibrate our ice-weighing machine.

Beyond GPS. Ice mass changes in the polar ice sheets are being monitored using a variety of remote sensing systems including airborne Light Detection And Ranging (LIDAR), space-based laser and radar altimeters, radar interferometers, and GRACE. In contrast, GNET makes in situ measurements at a limited number of points. GRACE and GPS both sense ice mass changes directly, whereas the other techniques measure changes in the height of the ice sheet surface. The relationship between height

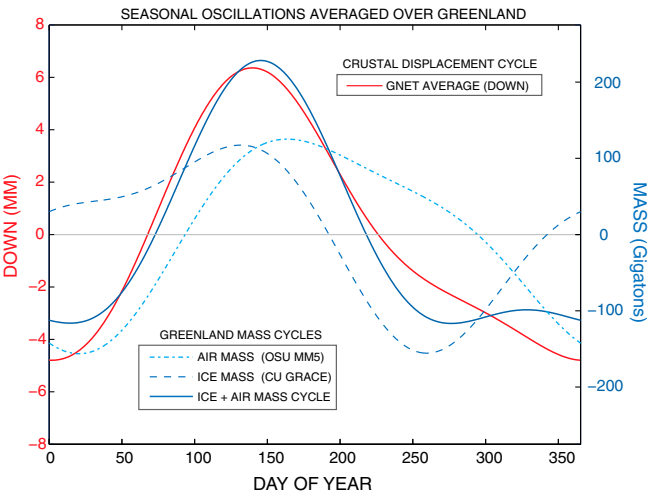

Fig. 6. A comparison of crustal displacement and surface loading cycles in Greenland. We plot the down (D) rather than up (U) component of displacement to aid the comparison with load cycles, since the ground moves down as the load increases. The seasonal cycles of the air mass and ice mass (overlying Greenland as a whole) are shown, as is their sum, which far better correlates with the displacement cycle.

change, H(t), and mass change, M(t), is complicated by the fact that the near-surface density of snow, firn, and ice can vary in space and in time (18). However, the surface-sensing techniques have much better spatial resolution than does GRACE or GPS. Clearly the best prospect is to combine all of these observations, using the strengths of each system to compensate for the weaknesses in the others. Even though GRACE and GPS measurements both sense M(t), they are complementary in that they have distinct spatial sensitivity kernels.

Discussion

GNET is clearly sensing ice loss at subannual, annual (i.e., seasonal), and multiyear timescales. Because a great many GNET stations are located in the near-field of these load changes, the earth's response will be sensitive to the elastic structure of the upper and lower crust (19, 20), which is much more variable than deeper earth structure and is not well known in Greenland. Recently installed seismic networks will soon help in this regard. It is probably inappropriate to use elastic-loading Green's functions based on the Preliminary Reference Earth Model (21), or any other radially symmetric, whole-earth model, in order to invert the crustal displacements observed by GNET for the spatial variation of surface load changes. At a minimum, we need to tune our Green's functions to the average elastic structure underlying GNET. We suspect that this last step will prove to be the thorniest problem associated with realizing Hager's (1) vision of weighing the ice sheets using GPS. However, as noted above, the demonstrated sensitivity of crustal displacement to atmospheric pressure variations, though at first glance an unwelcome complication, should provide us with the means to calibrate our Green's functions, and thus our weighing machine, by comparing daily GPS displacement time series with daily pressure fields from numerical weather models.

The most rapidly uplifting stations in GNET are KUAQ (30.5 mm/yr) and MIK2 (24.0 mm/yr) near Kangerdlugssuaq Glacier (Fig. 1). Because these stations were established in 2009, these rates were probably strongly influenced (i.e., perturbed upwards) by the 2010 melting day anomaly. Thus these estimates might be viewed as being biased by a short-lived event. But GRACE and the oldest GPS stations reveal changes in mass rates at three- to ten-year timescales too. The competing view (22) is that given more and longer time series of accurate measurements we will find that ice mass (and crustal displacement) frequently change at short timescales and that, as with nontidal sea level change, ice mass variability is distributed over a significant range of temporal and spatial scales.

ACKNOWLEDGMENTS. GNET is a collaboration of Ohio State University, National Space Institute at the Technical University of Denmark, and the University of Luxembourg, and it receives technical support from UNAVCO Inc. and logistical support from CH2M HILL Polar Services. The American component of GNET was funded by the US National Science Foundation though Grants ARC-0632320 and 1023566. We thank R. Simmon of the NASA Earth Observatory for providing us with the 2010 melting day anomaly map used in Fig. 5.

1. Hager B (1991) Weighing the ice sheets using space geodesy: A way to measure changes in ice sheet mass. *Eos. Trans. AGU* 72(Spring Meeting Suppl):71.
2. Velicogna I, Wahr J (2006) Measurements of time-variable gravity show mass loss in Antarctica. *Science* 311:1754–1756.
3. Bevis M, et al. (2009) Geodetic measurements of vertical crustal velocity in West Antarctica and the implications for ice mass balance. *Geochem Geophys Geosyst*, 10.1029/Q1005.
4. Tapley BD, Bettadpur S, Ries J, Thompson PF, Watkins MM (2004) GRACE measurements of mass variability in the Earth system. *Science* 305:503–505.
5. Le Meur E, Huybrechts P (2001) A model computation of the temporal changes of surface gravity and geoidal signal induced by the evolving Greenland ice sheet. *Geophys J Int* 145:835–849.
6. Peltier R (2004) Global glacial isostacy and the surface of the ice-age Earth: The ICE-5G (VM2) model and GRACE. *Annu Rev Earth Planet Sci* 32:111–149.
7. Paulson A, Zhong S, Wahr J (2007) Inference of mantle viscosity from GRACE and relative sea level data. *Geophys J Int* 171:497–508.
8. Simpson MJR, Wake L, Milne GA, Huybrechts P (2011) The influence of decadal- to millenial-scale ice mass changes on present-day vertical land motion in Greenland: Implications for the interpretation of GPS observations. *J Geophys Res*, 10.1029/B02406.
9. Wang H, Wu P, van der Wal W (2008) Using postglacial sea level, crust velocities and gravity-rate-of-change to constrain the influence of thermal effects on mantle heterogeneities. *J Geodyn* 46:104–117.
10. Khan SA, et al. (2007) Elastic uplift in southeast Greenland due to rapid ice mass loss. *Geophys Res Lett* 34:L21701.
11. Khan SA, Wahr J, Bevis M, Velicogna I, Kendrick E (2010) Spread of ice mass loss into northwest Greenland observed by GRACE and GPS. *Geophys.Res Lett* 37:L06501.
12. Jiang Y, Dixon TH, Wdowinski S (2010) Accelerating uplift in the North Atlantic region and an indicator of ice loss. *Nat Geosci* 3:404–407.
13. Tedesco M, et al. (2011) The role of albedo and accumulation in the 2010 melting record in Greenland. *Environ Res Lett* 6:014005.
14. Howatt I, et al. (2011) Mass balance of Greenland's three largest outlet glaciers. *Geophys Res Lett* 37 L12501.
15. Dong D, Fang P, Bock Y, Chang M, Miyazaki S (2002) Anatomy of apparent seasonal variations from GPS-derived site position time series. *J Geophys Res*, 10.1029/2001JB000573.
16. Van den Broeke M, et al. (2009) Partitioning recent Greenland mass loss. *Science* 326:984–986.
17. Box JE, et al. (2006) Greenland ice sheet surface mass balance variability (1988–2004) from calibrated Polar MM5 output. *J Clim* 19:2783–2800.
18. Helsen M, et al. (2008) Elevation changes in Antarctica mainly determined by accumulation variability. *Science* 320:1626–1629.
19. Bevis M, Kendrick E, Cser A, Smalley R (2004) Geodetic measurement of the local elastic response to the changing mass of water in Lago Laja, Chile. *Phys Earth Planet Inter* 141:71–78.
20. Bevis M, et al. (2005) Seasonal fluctuations in the mass of the Amazon River system and Earth's elastic response. *Geophys Res.Lett* 32:L16308.
21. Dziewonski A, Anderson DL (1981) Preliminary Reference Earth Model. *Phys Earth Planet Inter* 25:297–356.
22. Rignot E, Thomas R (2002) Mass balance of polar ice sheets. *Science* 297:1502–1506.

1. **Geodetic Analysis**.

We used GAMIT/GLOBK software to perform a daily GPS analysis of up to 700 stations per day from the mid 1990s to early 2011. Most of this data was obtained from the Data Centers of the International GNSS Service. Since GPS stations are established and terminate at different times, this required us to analyze a total of ~ 1,770 GPS stations. We allowed the orbital solutions that we used to relax so as to promote the overall geometrical consistency of our solutions. This analysis was loosely constrained to the reference frame ITRF2008. In order to define a geometrical reference frame especially geared to the

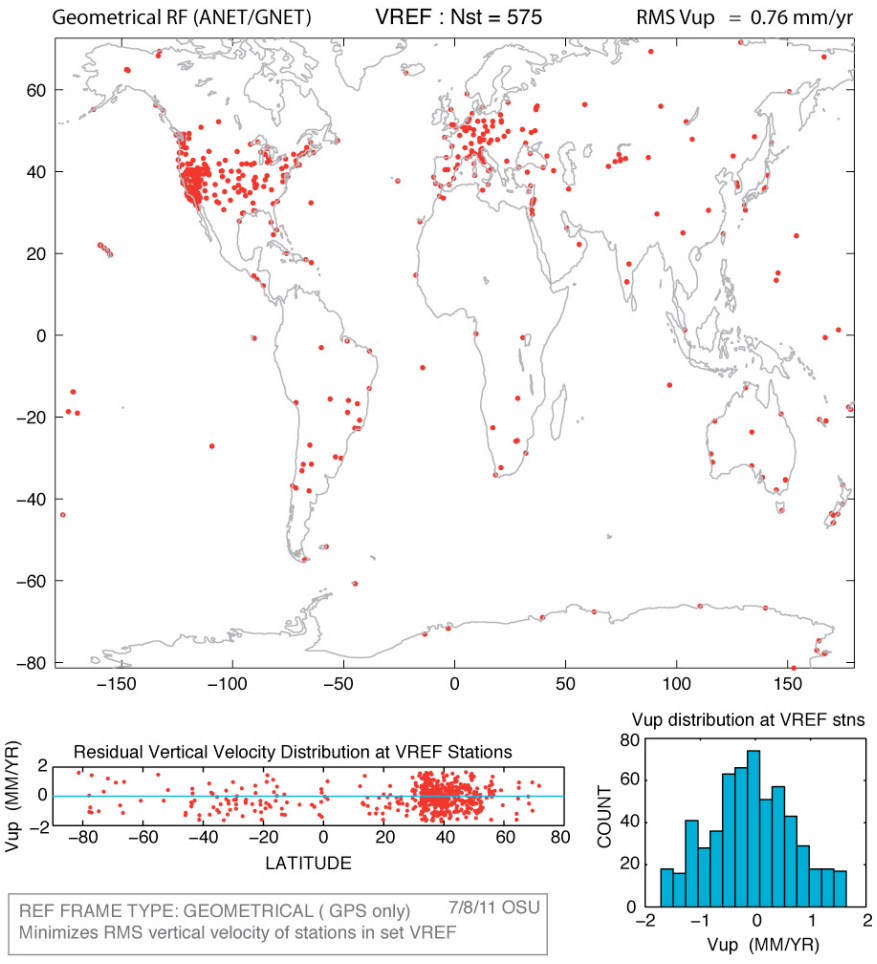

Figure S1. The spatial distribution of the GPS stations in the set VREF used to define the GNET reference frame, and the distribution of the vertical velocities of the VREF stations in toto, and as a function of station latitude, within this frame.

problem of characterizing vertical velocities for GNET and its sister network ANET in Antarctica, we transformed our solutions into a frame which minimizes the vertical velocity of 575 GPS stations (Figure S1). The RMS residual vertical velocity of the 575 stations in this frame is 0.76 mm/yr, and no station has a velocity outside the range -1.8 to + 1.8 mm/yr. There is no significant latitudinal trend of the VREF station velocities in this purely geometrical frame.

The velocities of the GNET stations in this frame are listed in Table S1, along with pertinent metadata, and are depicted in Figures 1 - 3. The entire velocity field is also shown in a single map in Figure S2. The formal standard error estimates for station velocity in Table S1 take into account that GPS time series have a colored noise spectrum (*23*). That is, these error estimates have been subject to a 'red noise correction'.

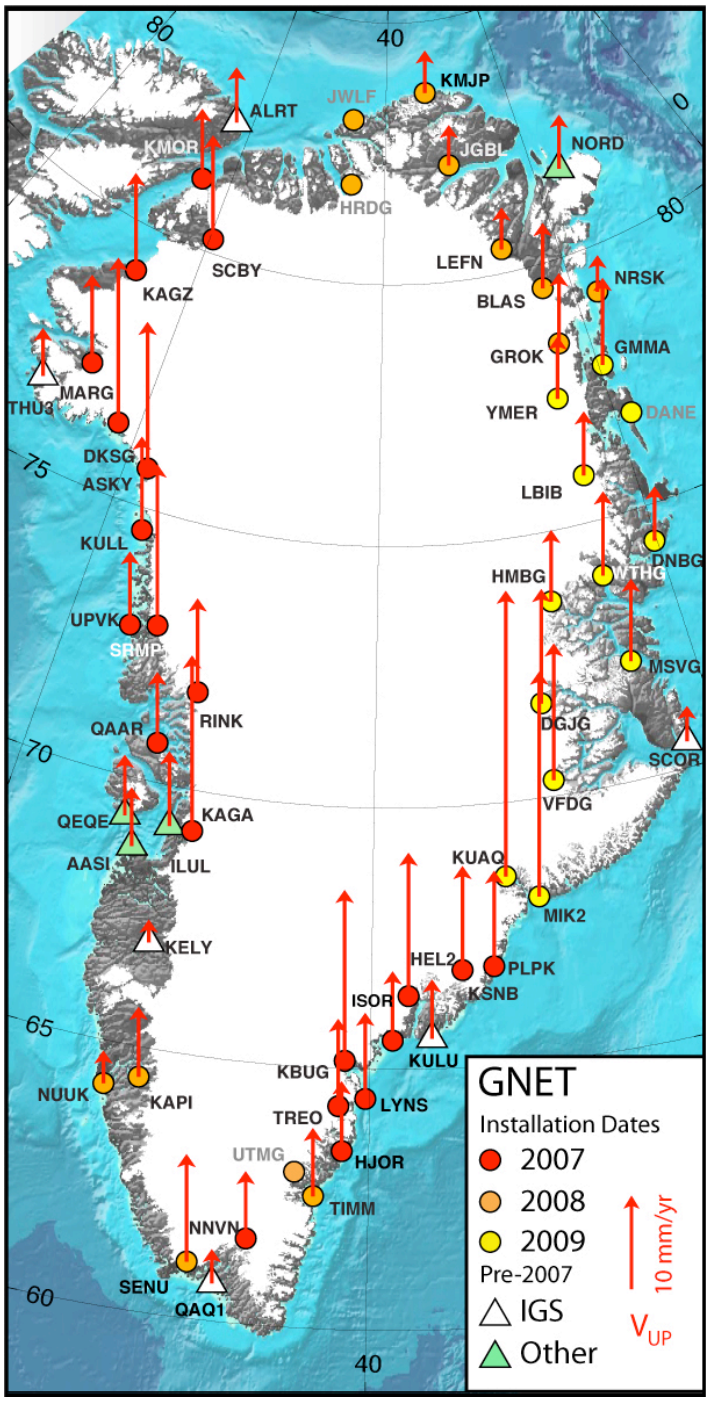

Figure S2. The vertical velocities of the GNET stations in the GNET reference frame. With the exception of stations THU2 and KULU all these results are based on a constant-velocity trend model, and indicate the solution obtained using all available data from 2000.0 to 2011.25. We used quadratic and cubic trend models at THU2 and KULU, so their model velocity varies with time (see Fig. 1), so we show and list their average vertical velocities. The standard errors associated with these solutions are almost always very small compared with the velocity estimate itself, as can be seen in Table S1. The lateral gradients in uplift velocity can be seen more clearly in Figures 1 - 3. Note that THU2 and THU3 refer to the same GPS antenna (but distinct GPS receivers).

We noted in the main text of this work that while the secular displacement trend at nearly all GNET stations is linear in time, we can model accelerating displacement trends using a polynomial model. Since this class of trend model rarely appears in the geodetic literature, we present it here:

$$\mathbf{x}_{\text{trend}} = \sum_{i=1}^{n_P+1} \mathbf{p}_i (t - t_R)^{i-1} \qquad (1)$$

This vector equation can be thought of as three scalar equations - one for each position coordinate. Vector **x** is the position vector of the GPS station, t is time, t_R is the reference time for the station (a conventional quantity which we equate to the mean epoch of measurement), n_p is the maximum power or order of the polynomial, and the $\mathbf{p}_i$ are the model coefficients. If n_p =1 this trend model reduces to the standard 'constant velocity model' in which $\mathbf{p}_1$ is the reference position and $\mathbf{p}_2$ is the station velocity vector. Setting n_p = 2 invokes the 'constant acceleration model', in which the acceleration vector is given by $2\mathbf{p}_3$. No matter what the value of n_p, $\mathbf{p}_1$ is always the reference position for the station, i.e. the value of $\mathbf{x}_{\text{trend}}$ when $t = t_R$.

Note that Eq. 1 refers only the trend model, and it is necessary to add a 4-term Fourier series to this trend (ref. *15*) in order to account for annual oscillations of the ground (Fig. 1).

2. **Comparison with PGR predictions**.

Nearly all PGR models (*5-9*) predict that most of the land surface exposed around the Greenland ice sheet is uplifting at a rate of -2 to + 3 mm/yr, though they disagree on the details. For example, ICE5G VM2 (*6*) predicts strong localized subsidence in SW Greenland, mild localized subsidence in SE Greenland, uplift everywhere else but stronger than normal uplift in NE Greenland. The more recent model Huy2 (*8*) predicts subsidence in the SW and uplift in the NE, but the amplitudes of the peak positive and negative velocities are significantly reduced. That is, Huy2 tends to predict PGR rates for coastal Greenland which are closer to zero than the predictions of ICE5G VM2 (*8*)**.**

We now present a formal comparison of the GNET velocities with those predicted by the PGR model ICE5G VM2 at the locations of the GNET stations. The median PGR rate predicted at the set of GNET stations is -0.6 mm/yr. Fifty percent of these predictions (i.e. those between the 25% and 75% percentiles) lie in the range -1.5 to + 2.0 mm/yr, and 75% of the predictions lie in the range -1.8 to + 3.9 mm/yr. In comparison the median observed uplift rate at the GNET stations is 7.7 mm/yr. The empirical cumulative distribution functions (CDFs) for the predicted PGR rates, the observed GPS velocities, and their difference is shown in Fig. S3. The differences (O-P) between GPS velocity and predicted PGR rates at the set of all GNET stations have a median value of 8.2 mm/yr. The corresponding interquartile range is 5.3 to 11.8 mm/yr, and the range of (GPS-PGR) velocities between the 12.5 and 87.5 percentiles (comprising 75% of GNET stations) is 2.4 to 17.0 mm/yr.

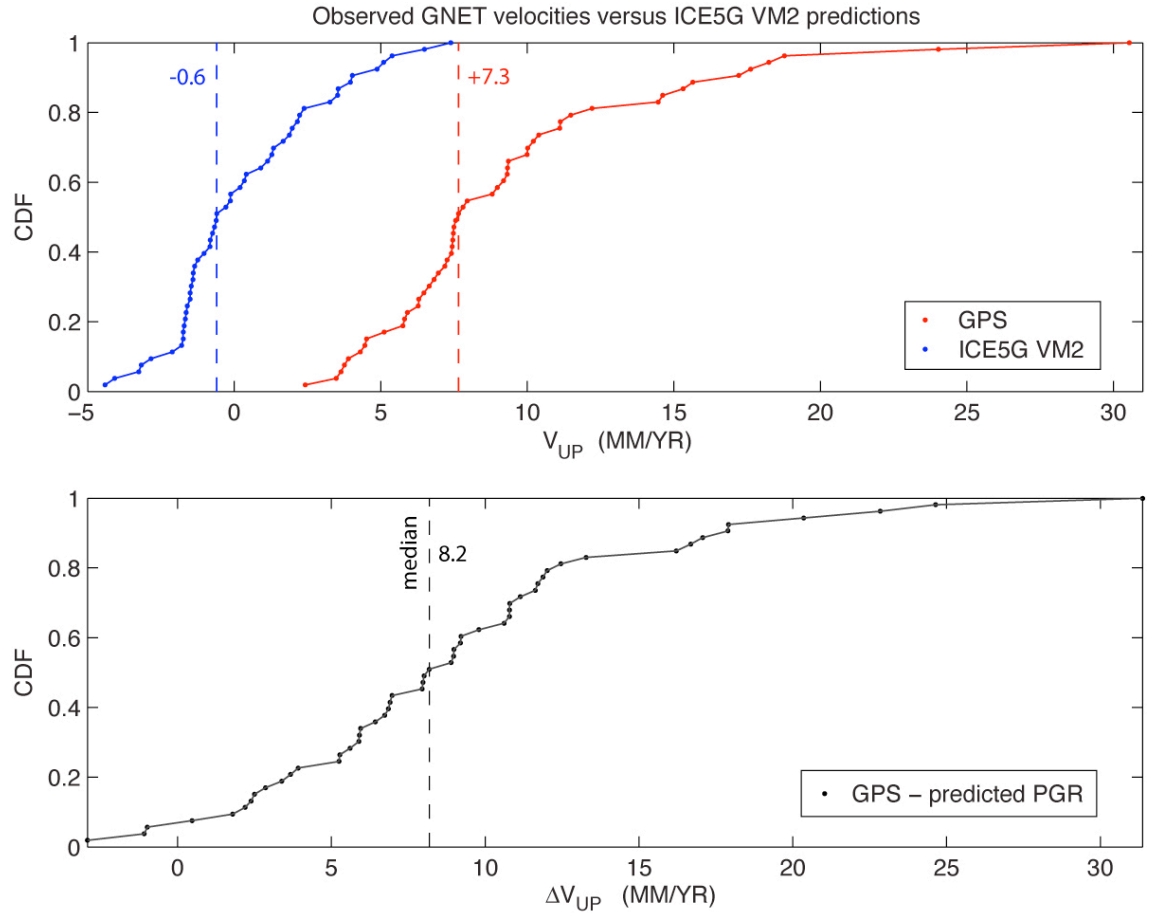

Figure S3. The upper plot shows the empirical CDFs for observed GPS velocities (red curve) and PGR rates predicted by ICE5G VM2 (blue curve) at the GNET stations. The lower plot shows the empirical CDF for the velocity difference (GPS - predicted PGR). Dashed vertical lines indicate population medians.

Clearly, the observed uplift rates are larger, usually much larger and sometimes very much larger than the PGR rates predicted by ICE5G VM2. This implies that the velocities observed by GNET are dominated by elastic rebound.

In NW and SE Greenland the observed coastline-perpendicular gradients in uplift rate are typically 3 - 10 times larger than those predicted by PGR models. This is not true in NE Greenland, where uplift rates vary little from one station to the next, but neither is this finding in close accord with the predictions of any leading PGR model.

Prior to the onset of the 2010 melting day anomaly the vertical velocities at stations NUUK and KAPI in SW Greenland were statistically indistinguishable from zero or slightly negative, providing some measure of support for the notion of long term subsidence in SW Greenland, a feature predicted by every PGR model based on the ICE5G ice history.

The GPS results are presented in a frame of reference that is defined using a purely geometrical criterion, whereas the PGR models are, in principle at least, associated with a center of mass frame. We cannot explain much of the discrepancy between the observed and predicted PGR uplift rates (Fig. S3) by invoking relative vertical motion of the two frames. Firstly, it is very unlikely that such a frame velocity bias is much larger than ~ 1 mm/yr. Secondly, the observed variation of vertical velocity is much larger than the spatial variation of the PGR rate predictions, and the spatial variability of uplift rate (as opposed to its absolute value) is nearly insensitive to frame drift. The same is true of the coastline perpendicular gradients in uplift rate. Lastly, we note that most published PGR models make quite disparate predictions for uplift rate, so it would be presumptuous to imagine that any of them can really be used to define a center of mass frame with better than ~ 1 mm/yr stability. The geometrical frame used in this study has the advantage of being robust. We can randomly remove 25 - 50 stations from the set VREF (Fig. S1) and in the great majority of cases very little change would occur in the vertical velocity solutions for GNET.

3. **The 2010 mass change anomaly from GRACE**

As described in the main text, we estimated the mass anomaly from GRACE using procedures as close as possible to those associated with our analysis of the uplift anomaly,

modifying the details of the process only slightly so as to accommodate the poorer time resolution associated with GRACE time series, and the somewhat higher temporal scatter than occurs (with monthly averaging) in these solutions. The mass time series, M(t), for 'North' and 'South' Greenland, we obtained at the University of Colorado using the sensitivity kernels depicted in Figure S4. The dividing line between the northern and southern domains is at the parallel 72.2° N.

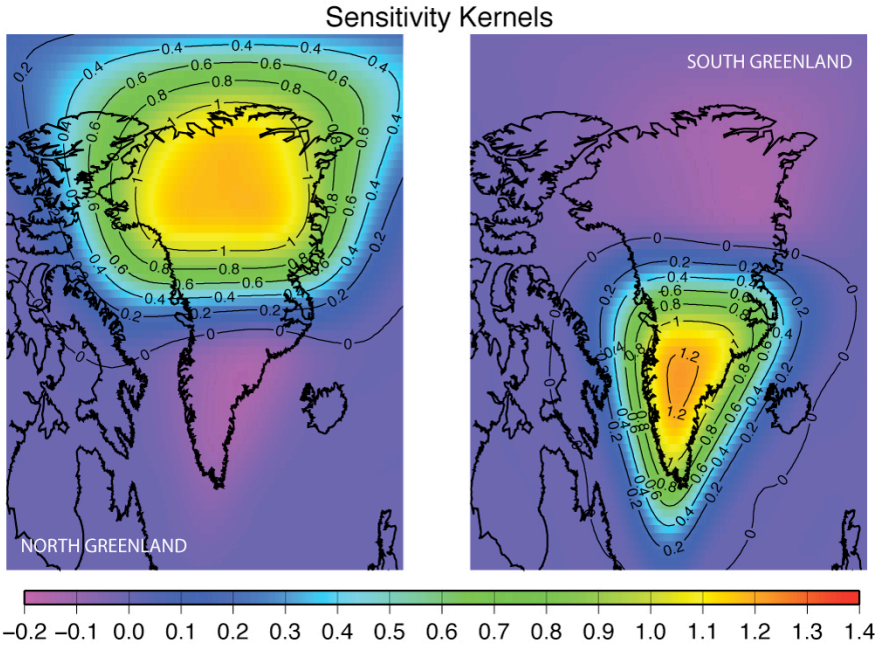

Figure S4. The sensitivity kernels used to isolate the mass time series for North and South Greenland. Note that these tend to slightly overweight the interior of the Ice Sheet, and slightly underweight its margins.

The 2010 mass anomaly is computed using a very similar procedure to that we used to estimate the uplift anomalies (Fig 4B). This procedure is illustrated in Figure S5 and explained in its caption. The resulting estimates for anomalous mass change in 2010 are -113 ± 28 GT in southern Greenland and +32 ± 28 GT in northern Greenland. The major loss in the south is clearly statistically significant, whereas the suggested minor gain in ice mass in the north is barely significant at the 2 sigma level.

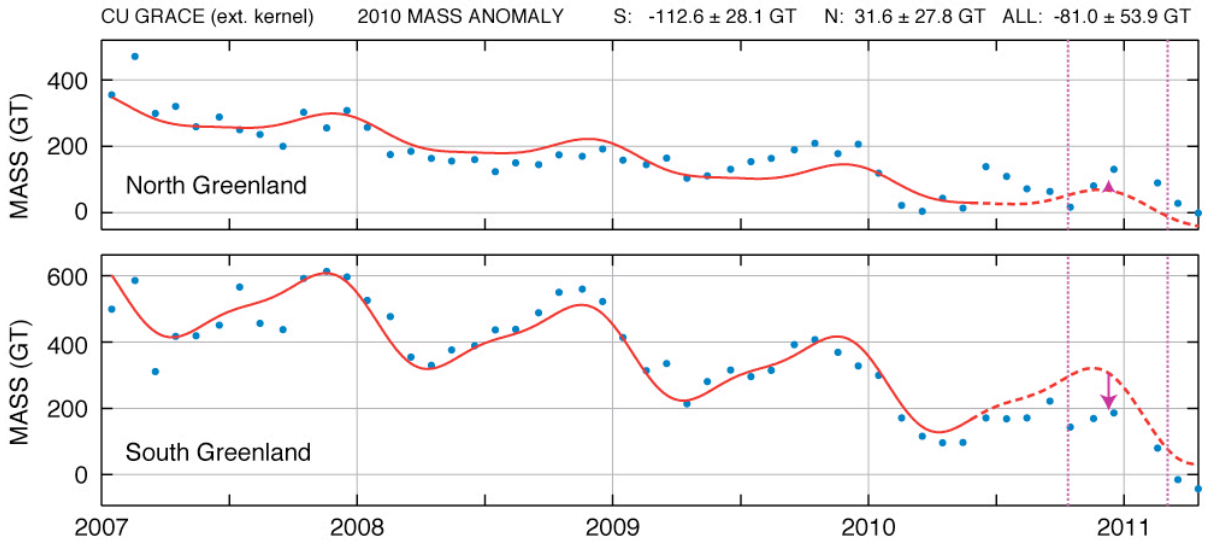

Figure S5. We fit a model composed of a linear trend plus a 4-term FS (solid red line) to each GRACE time series, M(t) (blue dots) for t < 2010.4, and then project that model forwards in time (dashed red line). The differences between this projected model and the actual observations are averaged in the time window 2010.78 - 2011.20 so as to form an estimate of the 2010 mass anomaly. These anomalies are depicted by the magenta arrows.

Table S1. GNET velocity solutions. The table columns are station code, station latitude and longitude, first and last epoch of observation, total time span (years), number of daily observations, the east, north and up components of velocity (mm/yr) and their standard errors (mm/yr), the correlation between the east and north velocity solutions. The penultimate column indicates if a constant velocity trend was used (1), or if higher order trend was invoked (0). If the latter, the velocities listed are the average velocities observed during the time span of observation. The symbol H indicates the members of HREF, the set of stations whose horizontal velocities were minimized so as to finalize the reference frame.

stnm	lat	long	t_first	t_last	tspan	nobs	Ve	Vn	Vu	Se	Sn	Su	Ren	cv?
AASI	68.719	-52.793	2006.048	2011.247	5.199	1419	0.16	0.19	6.28	0.12	0.14	0.19	0.029	1 H
ALRT	82.494	-62.340	2002.881	2011.247	8.366	2912	0.64	-2.05	5.91	0.07	0.07	0.12	0.003	1
ASKY	75.726	-58.257	2007.630	2010.160	2.530	911	-0.38	0.93	15.65	0.23	0.25	0.40	0.025	1
BLAS	79.539	-22.975	2008.515	2011.247	2.732	973	0.65	0.28	6.96	0.22	0.23	0.40	-0.019	1
DANE	74.312	-20.200	2009.619	2011.247	1.628	581	1.20	-0.16	5.82	0.48	0.53	0.82	-0.035	1
DGJG	71.787	-29.850	2009.608	2011.247	1.639	585	-0.76	0.78	12.21	0.43	0.48	0.72	-0.040	1
DKSG	76.352	-61.678	2007.635	2011.247	3.612	1252	0.95	1.55	17.62	0.14	0.15	0.24	0.027	1
GMMA	77.809	-19.652	2009.630	2011.122	1.492	531	1.00	-0.41	9.31	0.58	0.62	1.04	-0.025	1
GROK	78.443	-22.904	2008.515	2010.993	2.478	881	0.50	-0.75	7.49	0.26	0.28	0.46	-0.022	1
HEL1	66.401	-38.216	2006.654	2007.799	1.145	306	-1.74	0.90	14.47	1.10	1.24	1.68	-0.031	1
HEL2	66.401	-38.216	2007.643	2011.247	3.604	1287	-2.03	0.82	15.32	0.19	0.21	0.29	-0.036	1
HJOR	63.418	-41.148	2007.613	2011.247	3.634	1299	1.41	-0.00	7.44	0.19	0.21	0.27	-0.012	1
HMBG	73.676	-28.129	2009.611	2011.247	1.637	584	0.60	1.13	7.65	0.43	0.47	0.73	-0.037	1
ILUL	69.240	-51.061	2007.001	2011.245	4.243	1414	-0.50	0.41	7.95	0.11	0.13	0.18	0.023	1
ISOR	65.547	-38.975	2007.643	2010.643	3.000	908	-0.42	0.46	7.41	0.26	0.29	0.39	-0.034	1
JGBL	82.209	-31.004	2008.523	2011.242	2.719	968	1.42	0.16	4.30	0.23	0.23	0.41	-0.009	1
KAGA	69.222	-49.815	2006.392	2011.247	4.855	1623	-1.75	0.68	18.77	0.17	0.19	0.28	0.018	1
KAGZ	79.132	-65.853	2007.657	2011.247	3.590	376	0.53	0.06	10.39	0.21	0.23	0.38	0.019	1
KAPI	64.432	-50.271	2008.728	2011.247	2.519	710	0.13	0.38	7.47	0.37	0.42	0.55	0.025	1
KBUG	65.144	-41.158	2007.652	2011.247	3.596	1103	-1.08	-0.08	18.24	0.20	0.22	0.29	-0.018	1
KELY	66.987	-50.945	2000.001	2011.247	11.246	3332	0.33	-0.09	2.43	0.04	0.04	0.08	0.000	1 H
KMJP	83.643	-33.377	2008.537	2011.247	2.710	966	1.62	0.94	4.52	0.23	0.23	0.42	-0.005	1
KMOR	81.253	-63.527	2007.671	2011.247	3.577	1277	1.26	0.67	7.45	0.18	0.18	0.32	0.015	1
KSNB	66.863	-35.576	2007.633	2011.247	3.615	1297	0.33	1.54	11.11	0.18	0.20	0.27	-0.040	1
KUAQ	68.587	-33.053	2009.594	2011.247	1.653	589	-2.16	0.45	30.54	0.49	0.56	0.79	-0.043	1
KULL	74.581	-57.227	2007.619	2011.247	3.628	1295	-0.26	-0.18	9.99	0.13	0.14	0.23	0.027	1
KULU	65.579	-37.149	2000.001	2011.247	11.246	3629	-0.27	-0.50	6.30	0.06	0.06	0.11	0.000	0 H
LBIB	75.894	-23.853	2009.616	2011.247	1.631	582	0.35	-0.74	6.81	0.41	0.44	0.71	-0.030	1
LEFN	80.457	-26.293	2008.504	2010.124	1.620	577	0.74	-0.57	4.46	0.50	0.52	0.90	-0.015	1
LYNS	64.430	-40.198	2007.657	2011.247	3.590	1289	0.75	0.15	9.19	0.18	0.21	0.27	-0.019	1
MARG	77.187	-65.695	2007.660	2011.247	3.587	1288	0.92	0.92	9.36	0.13	0.14	0.23	0.026	1
MIK2	68.140	-31.452	2009.597	2011.247	1.650	589	0.21	-1.38	24.03	0.49	0.55	0.76	-0.038	1
MSVG	72.241	-23.913	2009.605	2011.247	1.642	586	1.52	0.32	8.80	0.39	0.44	0.66	-0.044	1
NNVN	61.632	-44.901	2007.616	2011.247	3.631	738	0.70	1.41	7.18	0.23	0.26	0.32	-0.005	1
NORD	81.600	-16.655	2006.717	2011.149	4.432	1239	0.63	-0.39	5.75	0.43	0.44	0.80	-0.011	1
NRSK	79.155	-17.725	2008.515	2010.695	2.180	777	1.83	-0.91	3.89	0.37	0.39	0.65	-0.020	1
NUUK	64.184	-51.731	2008.750	2011.247	2.497	775	-1.29	-0.89	3.48	0.45	0.51	0.67	0.034	1
PLPK	66.898	-34.033	2007.613	2011.184	3.571	1276	0.26	0.17	10.21	0.18	0.21	0.28	-0.046	1
QAAR	70.740	-52.688	2007.657	2011.247	3.590	1142	0.60	1.11	7.56	0.15	0.16	0.24	0.026	1
QAQ1	60.715	-46.048	2002.389	2011.247	8.858	3052	-0.22	0.14	3.64	0.06	0.07	0.09	0.006	1 H
QEQE	69.253	-53.522	2005.939	2011.247	5.309	1780	-0.28	0.50	6.47	0.08	0.09	0.13	0.031	1 H
RINK	71.848	-50.994	2007.660	2011.247	3.587	1288	3.16	2.21	10.01	0.16	0.17	0.26	0.018	1
SCBY	80.260	-59.594	2007.684	2009.865	2.180	527	1.23	-0.22	11.13	0.41	0.43	0.74	0.014	1
SCOR	70.485	-21.950	2005.089	2011.247	6.158	2135	0.58	-0.62	3.76	0.07	0.08	0.12	-0.049	1 H
SENU	61.070	-47.141	2008.373	2011.247	2.874	1028	-0.32	-0.32	11.48	0.33	0.38	0.46	0.013	1
SRMP	72.911	-54.394	2007.613	2011.247	3.634	1297	-1.22	-0.90	17.22	0.13	0.14	0.22	0.025	1
THU2	76.537	-68.825	2000.001	2011.247	11.246	3739	-0.17	-0.01	5.12	0.07	0.07	0.13	0.000	0 H
TIMM	62.536	-42.286	2007.630	2011.122	3.492	1246	0.98	1.29	7.27	0.20	0.23	0.29	-0.014	1
TREO	64.277	-41.375	2007.665	2011.247	3.582	1279	-0.50	1.01	9.33	0.20	0.23	0.30	-0.020	1
UPVK	72.788	-56.128	2007.417	2011.247	3.831	1353	-0.87	0.10	7.81	0.13	0.14	0.21	0.030	1
VFDG	70.300	-29.818	2009.600	2011.247	1.648	588	-0.06	1.58	14.62	0.44	0.50	0.72	-0.044	1
WTHG	73.955	-24.309	2009.613	2011.247	1.634	582	1.33	-0.17	8.98	0.43	0.48	0.74	-0.037	1
YMER	77.433	-24.326	2009.627	2011.247	1.620	577	0.37	-0.01	6.65	0.46	0.50	0.81	-0.025	1

Table S2. Estimates for the 2010 Uplift Anomaly (Ujmp) and its standard error (sigUj) in mm, for all GNET stations where it could be reliably estimated.

stnm	lat (N)	lon (E)	Ujmp	sigUj
AASI	68.719	-52.793	7.32	1.72
ALRT	82.494	-62.340	-1.86	2.11
BLAS	79.539	-22.975	4.57	1.72
DKSG	76.352	-61.678	-3.79	1.93
GROK	78.443	-22.904	8.51	2.10
HEL2	66.401	-38.216	15.09	1.72
HJOR	63.418	-41.148	12.55	1.68
ILUL	69.240	-51.061	6.34	1.53
JGBL	82.209	-31.004	1.16	1.72
KAGA	69.222	-49.815	12.89	1.59
KAPI	64.432	-50.271	13.24	1.59
KBUG	65.144	-41.158	3.24	1.70
KELY	66.987	-50.945	6.17	1.63
KMJP	83.643	-33.377	-1.12	1.75
KMOR	81.253	-63.527	-2.73	1.99
KSNB	66.863	-35.576	13.51	1.78
KULL	74.581	-57.227	-2.00	1.78
KULU	65.579	-37.149	10.72	1.58
LYNS	64.430	-40.198	9.27	1.68
MARG	77.187	-65.695	-1.37	1.74
PLPK	66.898	-34.033	13.68	1.75
QAAR	70.740	-52.688	3.74	1.76
QAQ1	60.715	-46.048	7.66	1.56
QEQE	69.253	-53.522	4.48	1.52
RINK	71.848	-50.994	6.62	1.78
SCOR	70.485	-21.950	4.13	1.70
SENU	61.070	-47.141	21.30	1.55
SRMP	72.911	-54.394	5.50	1.51
THU2	76.537	-68.825	-3.97	1.82
TIMM	62.536	-42.286	8.25	1.63
TREO	64.277	-41.375	14.59	1.93
UPVK	72.788	-56.128	1.78	1.61